Allergy Asthma Immunol Res. 2021 May;13(3):479-497
https://doi.org/10.4168/aair.2021.13.3.479
pISSN 2092-7355·eISSN 2092-7363

Allergy, Asthma & Immunology Research AAIR

Original Article

Check for updates

ATP6V0d2 Suppresses Alveoli Macrophage Alternative Polarization and Allergic Asthma via Degradation of PU.1

Na Liu[1,2†] **Yuchen Feng**[3†] **Huicheng Liu**[1] **Wenliang Wu**[3] **Yuxia Liang**[3] **Pingfei Li**[1] **Zhengping Wei**[1] **Min Wu**[1] **Zhao-Hui Tang**[4] **Junyan Han**[1] **Xiang Cheng**[5] **Zheng Liu**[6] **Arian Laurence**[7] **Huabin Li**[8] **Guohua Zhen**[3] **Xiang-Ping Yang**[1,2*]

[1]Department of Immunology, School of Basic Medicine, Tongji Medical College, Huazhong University of Science and Technology (HUST), Wuhan, China
[2]Department of Urology, Tongji Hospital, Tongji Medical College, Huazhong University of Science and Technology, Wuhan, China
[3]Division of Pulmonary and Critical Care Medicine, Department of Internal Medicine, Tongji Hospital, Tongji Medical College, Huazhong University of Science and Technology (HUST), Wuhan, China
[4]Department of Surgery, Tongji Hospital, Huazhong University of Science and Technology (HUST), Wuhan, China
[5]Laboratory of Cardiovascular Immunology, Institute of Cardiology, Union Hospital, Tongji Medical College, Huazhong University of Science and Technology (HUST), Wuhan, China
[6]Department of Otolaryngology-Head and Neck Surgery, Tongji Hospital, Tongji Medical School, Huazhong University of Science and Technology (HUST), Wuhan, China
[7]University College Hospital, NHS Trust, London, United Kingdom
[8]Department of Otolaryngology, Head and Neck Surgery, Affiliated Eye-Ear-Nose and Throat Hospital, Fudan University, Shanghai, China

ABSTRACT

Purpose: Macrophages are important regulators of environmental allergen-induced airway inflammation and asthma. ATP6V0d2 is a subunit of vacuolar ATPase highly expressed in macrophages. However, the functions of ATP6V0d2 in the regulation of pathogenesis of allergic asthma remain unclear. The aim of this study is to determine the function and related molecular mechanisms of macrophage protein ATP6V0d2 in allergic asthma.
Methods: We compared the disease severity between female C57BL/6 wild-type and *ATP6V0d2*$^{-/-}$ mice in an ovalbumin (OVA)-induced asthma model. We also investigated the association of expression of *ATP6V0d2*, *PU.1* and *CCL17* with disease severity among asthmatic patients.
Results: The expression of *ATP6V0d2* in sputum cells of asthmatic patients and in the lungs of OVA-challenged mice was enhanced compared to healthy subjects and their counterparts, respectively. However, *ATP6V0d2*-deficient mice exaggerated inflammatory cell infiltration as well as enhanced alternative activated macrophage (AAM) polarization and mucus production in an OVA-induced asthma model. Furthermore, we found that Atp6v0d2 promoted lysosomal degradation of Pu.1, which induced AAM polarization and Ccl17 production. Among asthma patients, *ATP6V0d2* expression was inversely associated with disease severity, whereas *PU.1 and CCL17* expression was positively associated with disease severity.
Conclusions: Our results identify macrophage Atp6v0d2, as an induced feedback inhibitor of asthma disease severity by promoting Pu.1 lysosomal degradation, which may in turn leads to reduced AAM polarization and Ccl17 production.

Keywords: Asthma; alveolar macrophage; V-type ATPase; Pu.1 protein

OPEN ACCESS

Received: May 18, 2020
Revised: Jul 20, 2020
Accepted: Sep 7, 2020

Correspondence to
Xiang-Ping Yang, PhD
Department of Immunology, School of Basic Medicine, Tongji Medical College, Huazhong University of Science and Technology (HUST), No. 13, Hangkong Road, Wuhan 430030, China.
Tel: +86-27-83692600
Fax: +86-27-83692608
E-mail: yangxp@hust.edu.cn

†Na Liu and Yuchen Feng contributed equally to this paper.

ORCID iDs
Na Liu
https://orcid.org/0000-0001-9903-1314
Arian Laurence
https://orcid.org/0000-0003-0942-8292
Huabin Li
https://orcid.org/0000-0002-9837-2405
Guohua Zhen
https://orcid.org/0000-0001-5582-7900
Xiang-Ping Yang
https://orcid.org/0000-0001-9003-1772

Disclosure

There are no financial or other issues that might lead to conflict of interest.

INTRODUCTION

Asthma is a chronic inflammatory disease of the lower airways of the lungs characterized by bronchospasm and inflammatory infiltration.[1,2] Macrophages are the most abundant immune cell type in the lungs and play crucial roles in environmental allergen-induced airway inflammation and asthma.[3,4] Alveolar macrophages (AMs) are the major effector cells of immune responses in the lungs, which process both proinflammatory and anti-inflammatory properties.[5,6] In allergic asthma, after allergen exposure there is a rapid recruitment of monocytes to the airways and lung tissues,[7] which differentiate into a subpopulation of AMs called monocyte-derived AMs (Mo-AMs).[8] Mo-AMs undergo further polarization and promote acute inflammatory responses.[9,10]

Despite its oversimplification and limitation in explaining all macrophage phenotypes and functions, polarized macrophages can be divided into classic activated macrophages (CAM) or alternative activated macrophages (AAMs) cell lineages.[11,12] AAM polarization is driven by cytokines involved in Th2 responses including IL-4 and IL-13. The ETS family transcriptional factor Pu.1 plays critical roles in macrophage differentiation and promotes AAM polarization.[13] Inducible ablation of Pu.1 attenuated eosinophil infiltration and airway hyperinflammation, which can be reversed by adoptive transfer of wild-type (WT) macrophages.[14,15] AAMs express Th2-related chemokines, CCR4 ligands such as Ccl17 and Ccl22 the latter of which has been reported to be induced by Pu.1.[16] In keeping with their association with atopic disease and Th2 associated cytokines, AAMs were significantly increased in bronchoalveolar lavage fluid (BALF) from patients with asthma and promoted the allergic airway responses and the pathogenesis of asthma.[17] Understanding the molecular details of regulation of AAM polarization and functions will provide a new insight into the treatment of asthma.

Atp6v0d2 is a subunit of vacuolar ATPase that acts as a proton pump and regulates extracellular and intracellular organelle acidification such as lysosome.[18,19] However, Atp6v0d2 is dispensable for the acidification for lysosomes in macrophages.[20] We recently identified that Atp6v0d2 senses inflammatory stimuli and tumor cell-derived lactate and regulates AAM differentiation in inflammation and tumor microenvironment.[21] In addition, Atp6v0d2 regulates leucine-induced mTORC1 activation and suppresses AAM polarization.[22]

Given the sentinel role of Atp6v0d2 in macrophages, we speculated that Atp6v0d2 might regulate macrophage-associated allergic asthma. Using sputum samples from asthmatic patients and *ATP6V0d2*$^{-/-}$ mice in an ovalbumin (OVA)-induced asthma model, we identified a novel ATP6V0d2-PU.1-CCL17 axis that regulates asthma pathogenesis and provided the mechanism that Atp6v0d2 mediates the lysosomal degradation of Pu.1, which directly binds to the *Ccl17* promoter and regulates the expression of Ccl17. More importantly, ATP6V0d2 expression was reversely associated with disease severity in human asthmatic patients.

MATERIALS AND METHODS

Mice

ATP6V0d2$^{-/-}$ mice were generated using transcription activator-like effector nuclease (TALEN) technology as previously described.[21] C57BL/6 WT mice were purchased from Huafukang (Beijing, China). All the mice were bred and housed in a specific-pathogen-free facility at

https://doi.org/10.4168/aair.2021.13.3.479

Tongji Medical College, Huazhong University of Science and Technology (Wuhan, China) and used in accordance with institutional guidelines.

Patients and specimens

Induced sputum samples were obtained from healthy volunteers (n = 16) and asthmatic patients (n = 22) enrolled in Tongji Hospital. All of the subjects provided informed consent. The diagnosis of asthma was based on asthma guidelines provided by the American Thoracic Society.[23] None of the patients in the asthma group had undergone inhaled corticosteroid therapy before blood and lung function tests. All studies with human subjects were approved by the Institutional Ethical Review Board of Tongji Hospital (TJ-IRB20180518). The clinical characteristics of all subjects are provided in **Supplementary Table S1**.

Sputum induction and sputum cell isolation

Sputum induction was performed as described before.[24] In brief, the sputum was induced in healthy volunteers and asthmatic patients by inhalation of nebulized hypertonic (4.5%, 25 mL) sterile saline solution. Patients expectorated whenever it is needed or every 5 minutes. If sputum amount was inadequate, induction was continued for another 5 minutes. The whole procedure lasted for 20 minutes. The sputum was isolated from saliva and dispersed with 0.1% dithiothreitol and then filtered through a 40-μm Nitex filter to remove mucus. The resulting suspension was centrifuged at 1,000 rpm for 5 minutes at 4°C and the cell pellets were washed once and re-suspended with phosphate buffered saline (PBS). The cell suspension was centrifuged by a cytospin for immunohistochemistry staining or was used directly for RNA isolation or flow cytometry analysis.

Murine bone marrow-derived macrophage (BMDM) induction and activation

Primary BMDMs were generated by culturing mouse bone marrow cells in RPMI 1640 medium supplemented with 10% fetal calf serum, 100 U/mL penicillin G and 100 μg/mL streptomycin, in addition to recombinant mouse M-CSF (20 ng/mL, PeproTech, Rocky Hill, NJ, USA) for 7 days. On day 7, macrophages were washed and stimulated with IL-4 (20 ng/L, PeproTech) for different hours.

Quantitative reverse transcription polymerase chain reaction (RT-PCR)

Total RNAs were extracted from lung tissues or cells with Trizol reagent (Invitrogen, Carlsbad, CA, USA). cDNA was synthesized with 1 μg RNA isolated from mouse lung tissues or with 0.3 μg RNA from human sputum samples by using the Reverse Transcription Kit (Toyobo, Osaka, Japan) following the manufacturer's protocol. All quantitative RT-PCR was performed with the SYBR green method on a Bio-Rad CFX. The quantification of the results was performed by the comparative Ct ($2^{-\Delta\Delta Ct}$) method. The Ct value for each sample was normalized by the value for *Gapdh or β-Actin* gene. Primer sequences for mouse genes and human genes were provided in **Supplementary Table S2**.

OVA-induced asthma model in mice

Asthma was induced in female WT and *ATP6V0d2*$^{-/-}$ mice (8–12 weeks old) as previously described.[25] Briefly, mice were sensitized by intraperitoneal injection of 100 μL OVA liquid in which 20 mg of OVA (grade V, Sigma, A5503; Sigma-Aldrich, St. Louis, MO, USA) was emulsified in 4 mg of aluminum hydroxide (Sigma, 239186; Sigma-Aldrich) in a total volume of 100 mL on days 0, 7, and 14. Mice were injected with an equal volume of saline served as control animals. After sensitization, 1% OVA (grade II, Sigma, A5253; Sigma-Aldrich) was atomized and inhaled by mice for 7 consecutive days to induce asthma.

https://doi.org/10.4168/aair.2021.13.3.479

Lung tissue histological analysis

For histological analysis, lungs were harvested and fixed in 4% buffered formalin for 24 hours at room temperature. Tissues were then embedded in paraffin; 6-μm sections were cut with a micrometer and stained with hematoxylin and eosin, Periodic acid-Schiff (PAS) and Masson. The images were assessed by 2 independent pathologists using a bright field microscope in a blinded fashion. Inflammatory cell infiltration was scored with a scale of 0 to 4, with 0 representing no inflammation, 1 representing light cell infiltration in only a few areas, 2 and 3 representing moderate cell infiltration encompassing < 20% and 50%, respectively, of the airways and vessels, and 4 representing dense cell infiltration encompassing > 50% of the airways and vessels. All histomorphometric measurements were quantified within 3 randomly selected visual fields per slide from each group (n = 4–6).

Flow cytometry

After perfusion with 5 mL of PBS through the right ventricle, lung tissues were cut into small pieces and digested with RPMI 1640 medium containing 1 mg/ml collagenase D (Roche, 11088866001; Roche, Basel, Switzerland) for 1 hour at 37°C. Single lung cell suspensions were obtained after filtration and red cell lysis. Before staining, cells were incubated with Fc blocker anti-CD16/32 (Biolegend, clone 93; Biolegend, San Diego, CA, USA). Cells were stained with the following surface anti-mouse antibodies: CD11b-FITC (clone M1/70), F4/80-Percp/cy5.5 (clone BM8), CD206-PE/cy7 (clone C068C2), CD3-APC/cy7 (clone 17A2), CD19-BV421 (clone 6D5) (all from Biolegend), SiglecF-PE (clone, 1RNM44N) and CD64-APC (clone 10.1) from eBioscience (San Diego, CA, USA).

For human sputum cell staining, the single cell suspensions were blocked with anti-human Trustain FcXTM (Biolegend), then stained with the following antibodies: CD33-FITC (clone HIM3-4), CD3-APC (clone OKT3), CD3-PE (clone HIT3a), CD19-APC (clone HIB19), CD68-PE (clone Y1/82A) (all from eBioscience), and CD68-APC (clone Y1/82A, Biolegend). Samples were collected on a BD Verse Flow cytometer, and data were analyzed using FlowJo software (Tree Star, San Carlos, CA, USA).

Immunofluorescence and immunoblotting

BMDMs were seeded at 3×10^4 cells per well on glass slides and rested overnight for proper attachment. Lung AMs from control mouse BALF were seeded at 1×10^4 cells per well on glass slides, and rested 3 hours for attachment. Then, the cells were stimulated with IL-4 (20 ng/mL) for the indicated time, followed by incubation with 1:5,000 PBS-diluted LysoTracker Red DND-99 dye (Cat: L7528, Life Technologies, Carlsbad, CA, USA) for 30 minutes. Afterwards, cells were washed twice with sterile PBS and fixed with 4% paraformaldehyde, permeabilized with 0.05% Triton X-100, and blocked in 5% BSA. Anti-Pu.1(2266, CST) was incubated overnight in 4°C. Secondary fluorescent antibodies FITC (from Life Technologies or Jackson Laboratories, Bar Harbor, ME, USA) were added for 1 hour and 4',6-diamidino-2-phenylindole (DAPI) was used for nuclear counterstaining. Samples were imaged with a SP5 confocal (Leica, Wetzlar, Germany) after 24-hour mounting. Immunoblotting was performed according to the standard method. Cell lysates were separated by sodium dodecyl sulfate-polyacrylamide gel electrophoresis and proteins were transferred from gel onto polyvinylidene difluoride membranes. Membranes were incubated with the following primary antibodies: anti-Atp6v0d2 (SAB2103221; Sigma), anti- Atp6v0d1 (ab56441; Abcam, Cambridge, UK), anti- Atp6v1a (ab137574; Abcam), p-NF-κb (3033; Cell Signaling Technology, Danvers, MA, USA), Pu.1 (2258; Cell Signaling Technology), Stat6 (5397; Cell Signaling Technology), phosphor-Stat6 (9362; Cell signaling Technology), p62 (PM045; MBL, Woburn, MA, USA), and β-actin (4970S; Cell Signaling Technology). After washing, membranes

https://doi.org/10.4168/aair.2021.13.3.479

were incubated with appropriate secondary horseradish peroxidase-conjugated antibodies, and then developed with enhanced chemiluminescence (GE Healthcare, Chicago, IL, USA).

Statistical analysis

All values are expressed as the mean ± standard error of the mean for each group. Statistical significance was assessed using an unpaired Student's *t*-test or Mann-Whitney *U* test. Using Prism software for data comparisons were made between 2 groups. When groups contained more than 2 samples, they were analyzed using one-way analysis of variance with Tukey's *post hoc* test. GraphPad Prism was used for all statistical calculation. A P value of < 0.05 was considered statistically significant (GraphPad, San Diego, CA, USA).

RESULTS

ATP6V0d2 expression is enhanced in the sputum cells of asthmatic patients as well as in lung tissue and BALF cells of OVA-induced asthmatic mice

To investigate the potential role of ATP6V0d2 in asthma, we first compared the mRNA expression of *ATP6V0d2* in the cell pellets of induced sputum from healthy donors and asthmatic patients. Asthmatic patients exhibited significantly higher *ATP6V0d2* mRNA expression in the sputum cells compared to healthy controls (**Fig. 1A**). This was confirmed at the protein level using immunohistochemistry in the sputum cells (**Fig. 1B and C**). Notably, the percentage of $CD68^+$ macrophage population was increased in the sputum of asthmatic patient (**Supplementary Fig. S1A**). Immunofluorescence data showed that the expression of ATP6V0d2 was mainly co-localized with CD68 staining in sputum cells from asthmatic patient (**Fig. 1D**). Similar to the human results, we found that OVA-challenged mice showed significantly higher expression of *Atp6v0d2* mRNA within lung tissues (**Fig. 1E**). Around 89% cells within BALF from control mouse were $F4/80^+CD11c^+$ AMs (**Supplementary Fig. S1B**). Similarly, *Atp6v0d2* expression was enhanced in the OVA-treated BALF cells compared to unchallenged controls (**Fig. 1F and G**). Taken together, these data demonstrate that ATP6V0d2 expression is enhanced in both asthmatic humans and mice.

IL-4 induces Atp6v0d2 expression via activation of Stat6 in macrophages

IL-4 is a major cytokine in driving Th2 differentiation and AAM polarization. The BALF supernatants of OVA-sensitized mice had significantly enhanced IL-4 production, compared to control mice (**Fig. 2A**). Stimulation of WT BALF cells with IL-4 enhanced *ATP6V0d2* mRNA expression (**Fig. 2B**). IL-4 induced *ATP6V0d2* mRNA expression and protein expression in BMDMs (**Fig. 2C and D**). However, IL-4 had no effect on the expression of Atp6v0d1 and Atp6v1a, suggesting that IL-4 specifically regulates Atp6v0d2 expression in macrophages. By sequence comparison, we identified 4 putative Stat6 binding sites in the *ATP6V0d2* promoter (**Fig. 2E**). Stimulation of IL-4 in macrophages led to enhanced Stat6 binding in the regions amplified by primer pairs 1, 2, and 3 (**Fig. 2F**). This was associated with enhanced trimethylation of histone 3 lysine 4 (H3K4me3), a transcriptional activation marker in the primer 1 region (**Fig. 2G**). While IL-4 promotes the AAM phenotype, lipopolysaccharide (LPS) induces macrophage polarization into CAM phenotype. Consistent with this, LPS suppressed Atp6v0d2 expression, but not Atp6v0d1 and Atp6v1a, in an NF-kB-dependent manner (**Supplementary Fig. S2A and B**). The suppression of IL-4-induced *Atp6v0d2* by LPS was dose-dependent (**Supplementary Fig. S2C and D**) and the addition of LPS resulted in significantly reduced Stat6 binding to the promoter (**Fig. 2H**). Conversely, increasing dose of IL-4 could overcome the suppressive effect of LPS on Atp6v0d2 expression (**Supplementary Fig. S2E and F**).

https://doi.org/10.4168/aair.2021.13.3.479

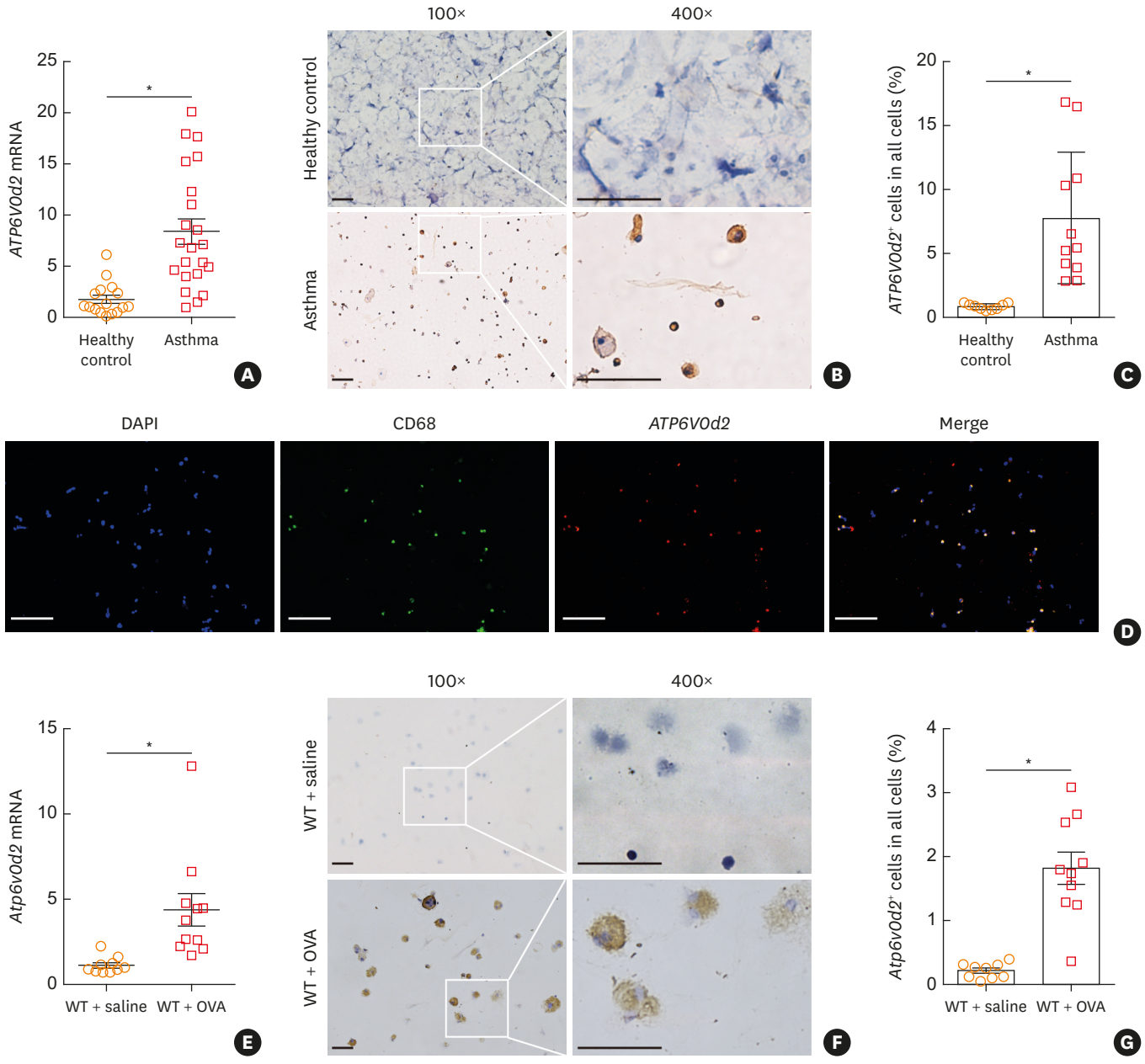

Fig. 1. *ATP6V0d2* expression is increased in the sputum cells of asthmatic patients and in the lung tissues and BALF cells of OVA-challenged mice. (A) qPCR analysis of *ATP6V0d2* expression in sputum samples from asthmatic patients (n = 22) and healthy controls (n = 16). (B, C) A representative image of IHC analysis of *ATP6V0d2* in the sputum samples from healthy donors and asthmatic patients as well as quantification of the percentages of *ATP6V0d2*-positive cells in each sputum sample in healthy controls and asthmatic patients. (D) Immunofluorescence staining of isolated sputum cells from asthmatic patients' saliva with DAPI (blue), anti-CD68 (green), and anti-*ATP6V0d2* (red). (E) The expression of *Atp6v0d2* in the lungs of mice after OVA sensitization (n = 10–11). (F, G) A representative image of IHC analysis of *Atp6v0d2* in the BALF between WT mice and OVA-induced mice and the percentages of *Atp6v0d2*-positive cells in BALF cells sample were analyzed (scale bar: 100 μm). The percentage of *ATP6V0d2* in sputum samples from human (n = 9–11) or in BALF from mice (n = 9–10) was analyzed by ImageJ software, and the mean value of 3 image fields per slides was plotted. Data are shown as the ratio compared to *Gapdh* or β-*ACTIN* to $2^{-\Delta Ct}$ for mRNA levels. Data were assessed by the Mann-Whitney *U* test and are presented as mean ± standard error of the mean.
BALF, bronchoalveolar lavage fluid; OVA, ovalbumin; qPCR, quantitative polymerase chain reaction; IHC, immunohistochemistry; DAPI, 4',6-diamidino-2-phenylindole; WT, wild-type.
*$P < 0.001$.

Taken together, these data demonstrate that Atp6v0d2 expression is counter-regulated by IL-4 and LPS, suggesting it may serve as a focal point for macrophage polarization and function.

https://doi.org/10.4168/aair.2021.13.3.479

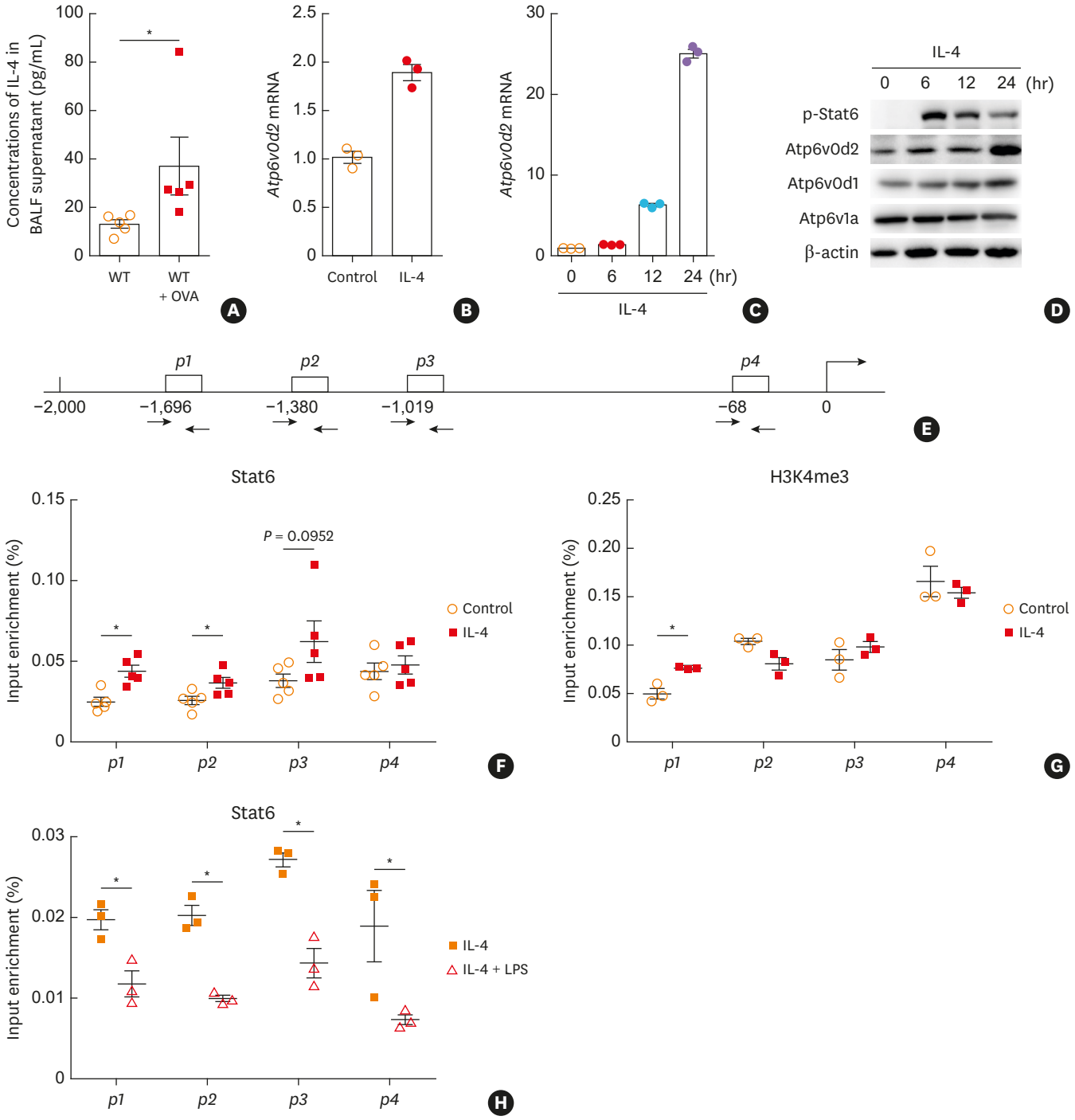

Fig. 2. *ATP6V0d2* expression is induced by IL-4 through activation of Stat6 in macrophages. (A) IL-4 concentrations were measured in control animals and OVA-treated mice. (B) BALF cells isolated form control mice were stimulated with IL-4 (20 ng/mL) for 3 hours and the expression of *Atp6v0d2* was detected by qPCR. (C) Macrophages were stimulated with IL-4 (20 ng/mL) for the indicated time and the expression of *Atp6v0d2* was determined by qPCR. (D) Immunoblotting of p-Stat6, Atp6v0d2, Atp6v0d1 and Atp6v1a in macrophages stimulated with IL-4 (20 ng/mL) for the indicated time. (E) Schematic representation showing primers used for the CHIP analysis. (F, G) Chromatin immunoprecipitation analysis of *Stat6* and *H3K4me3* occupancy to the *Atp6v0d2* locus in macrophages that were stimulated with IL-4 for 2 hours. Precipitated DNA was amplified by qPCR for primer sites *p1*–*p4* and results were presented relative to input DNA. (H) Chromatin immunoprecipitation analysis for *Stat6* occupancy to the *Atp6v0d2* locus in macrophages that were stimulated with IL-4 plus LPS (100 ng/mL) for 2 hours. Data are representative of 3 independent experiments. Data were assessed by unpaired Student's *t*-test and are presented as mean ± standard error of the mean. OVA, ovalbumin; BALF, bronchoalveolar lavage fluid; qPCR, quantitative polymerase chain reaction; LPS, lipopolysaccharide.
*$P < 0.05$; †$P < 0.01$; ‡$P < 0.001$.

https://doi.org/10.4168/aair.2021.13.3.479

ATP6V0d2-deficient mice exhibit exacerbated OVA-induced airway inflammation, remodeling and mucus production

To investigate the function of Atp6v0d2 in asthma, we employed an OVA-induced allergic asthma model in WT and *ATP6V0d2*-deficient mice. We found significantly enhanced infiltration of inflammatory cells surrounding the airway and blood vessels of the lungs in *ATP6V0d2*$^{-/-}$ mice compared with control mice (**Fig. 3A**). The inflammatory scores in the lungs of *ATP6V0d2*$^{-/-}$ mice were significantly higher (**Fig. 3B**). Using PAS staining, we found aggravated mucus hyperplasia in the bronchi in OVA-challenged *ATP6V0d2*$^{-/-}$ mice (**Fig. 3C and D**). Next, we used Masson trichrome staining of the collagen deposition to evaluate the airway wall thickening. The lungs of *Atp6v0d2*-deficient mice had enhanced collagen deposition (**Fig. 3E and F**). Moreover, the expression of *Muc5ac* and *Muc5b* was further potentiated in the lungs of OVA-challenged *ATP6V0d2*$^{-/-}$ mice despite the difference of *Muc5b* was not significant (**Fig. 3G and H**). Together, these data demonstrate that Atp6v0d2 suppresses OVA-induced airway inflammation, remodeling, and mucus production.

ATP6V0d2$^{-/-}$ mice enhance inflammatory cell infiltration and cytokine productions in OVA-induced asthma

Next, we compared the inflammatory cell infiltration in the BALF supernatants of OVA-challenged WT and *ATP6V0d2*$^{-/-}$ mice. *ATP6V0d2*$^{-/-}$ mice had significantly increased numbers of total infiltrated inflammatory cells compared to WT mice, and the numbers of eosinophils, macrophages, and T lymphocytes were higher in the BALF supernatants of *ATP6V0d2*$^{-/-}$ mice (**Fig. 4A**). Flow cytometry showed enhanced presence of SiglecF^{+}CD64^{-} eosinophils among the populations of CD11b^{+} cells in the lungs of *ATP6V0d2*$^{-/-}$ mice (**Fig. 4B**). T-cell infiltration in the lungs of *ATP6V0d2*$^{-/-}$ mice after OVA challenge was enhanced; however, the CD19^{+} B-cell infiltration was comparable (**Supplementary Fig. S3A**). Next, we compared the levels of type 2 cytokines involved in the asthma process in lung tissue homogenates as well as BALF of WT and *ATP6V0d2*$^{-/-}$ mice. OVA-challenged WT mice had elevated levels of IL-4, IL-5, IL-13, and Ccl17 in the lungs compared to control animals. The expressions of IL-4, IL-5, IL-13 and Ccl17 were significantly further enhanced in the absence of *ATP6V0d2* upon OVA challenge (**Fig. 4C**). Similar results were obtained for IL-4, IL-5, IL-13, and Ccl17 production in the BALF supernatants (**Fig. 4D**).

Despite the enhanced expression of IL-6 and IL-10 in WT mice after OVA treatment, the concentrations of IL-6 and IL-10 in the lungs were comparable between WT and *ATP6V0d2*$^{-/-}$ mice (**Supplementary Fig. S3B**). Similar results were obtained in the BALF (**Supplementary Fig. S3C**). Meanwhile, the serum levels of immunoglobulin E (IgE) and IgG1were also enhanced in *ATP6V0d2*$^{-/-}$ mice compared to control animals despite the difference of IgG1 was not significant (**Fig. 4E and F**). Taken together, these data demonstrate that *ATP6V0d2*-deficiency led to enhanced infiltration of eosinophils, macrophages and T lymphocytes type 2 cytokines as well as IgE production during asthma.

Deletion of *ATP6V0d2* results in enhanced AAM polarization in asthma

We next asked whether the enhanced asthma disease severity seen in the absence of Atp6v0d2 was due to enhanced alternative macrophage polarization. Immunofluorescence staining of lung sections after OVA-challenge showed the presence of higher numbers of F4/80^{+}CD206^{+}AAM cells in the group of *ATP6V0d2*$^{-/-}$ mice compared to WT mice (**Fig. 5A and B**). This was further confirmed by flow cytometry analysis in the lung tissues of OVA-treated *ATP6V0d2*$^{-/-}$ mice compared to WT mice (**Fig. 5C**). In the lungs of OVA-treated *ATP6V0d2*$^{-/-}$ mice, the expressions of AAM associated genes, including *Fizz-1*, *Mrc-1*, *Ym-1*, and *Il-4r,* were significantly higher compared

https://doi.org/10.4168/aair.2021.13.3.479

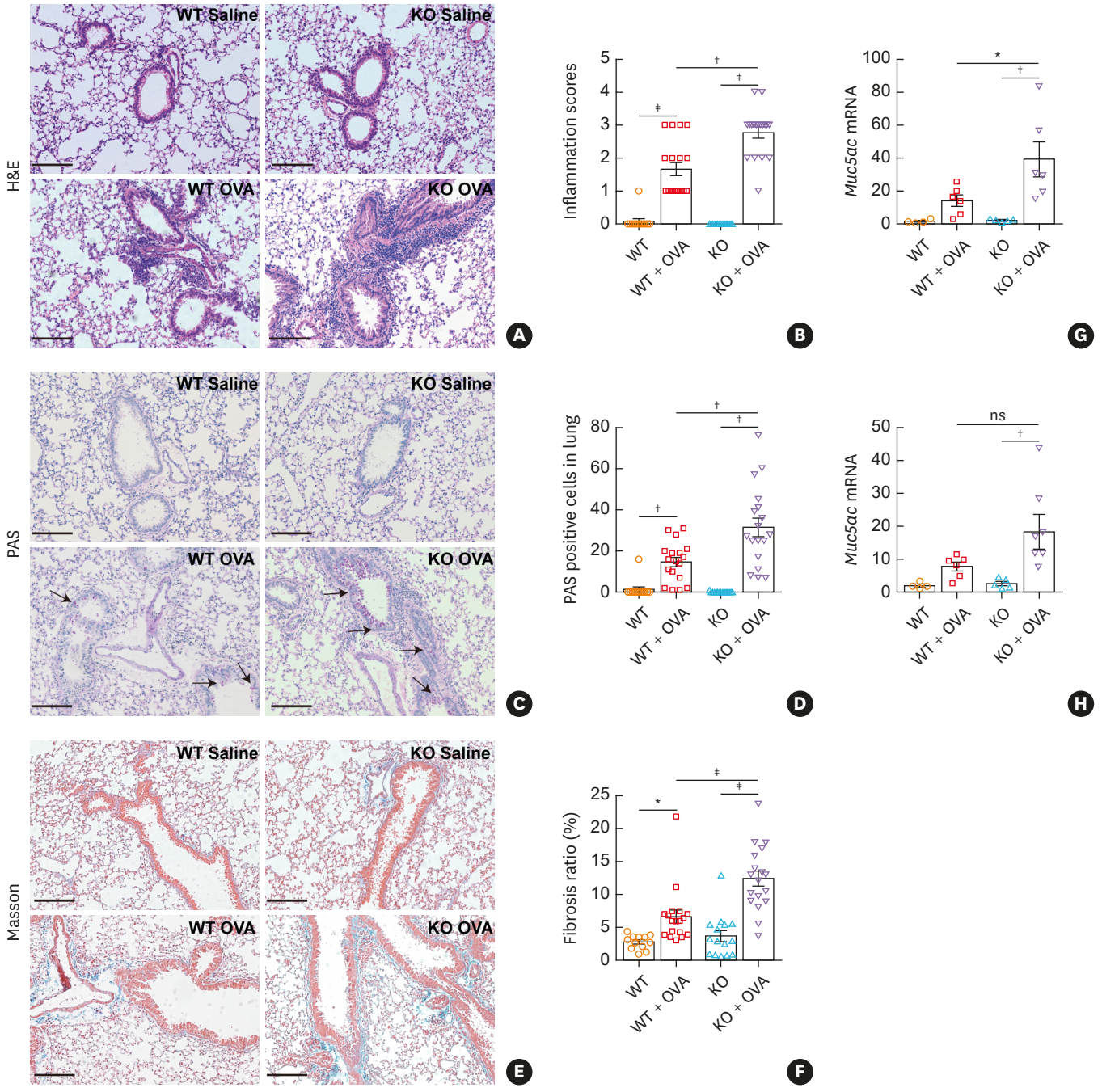

Fig. 3. *ATP6V0d2*-deficient mice were more susceptible to OVA-induced asthma. (A, B) Hematoxylin and eosin staining of lung tissues in WT and *ATP6V0d2*$^{-/-}$ mice after saline or OVA treatment, and the mean scores of inflammation were analyzed. (C, D) PAS staining on lung tissues in WT and *ATP6V0d2*$^{-/-}$ mice after saline or OVA treatment and the PAS-positive cells were counted. (E, F) Masson trichrome staining of lung tissues in WT and *ATP6V0d2*$^{-/-}$ mice after saline or OVA treatment, and the positive areas were quantified. (G, H) qRCR analysis of *muc5ac* and *muc5b* in the lung tissues from WT and *ATP6V0d2*$^{-/-}$ mice after saline or OVA treatment (scale bar: 100 μm). Data are representative of 2 independent experiments, and shown as the ratio compared to *Gapdh* to $2^{-\Delta Ct}$ for mRNA levels. Quantification was analyzed for 3 randomly selected visual fields per slide (n = 4–6). Data were assessed by one-way analysis of variance with Turkey's test and are presented as mean ± standard error of the mean.
OVA, ovalbumin; WT, wild-type; PAS, Periodic acid-Schiff; qPCR, quantitative polymerase chain reaction; KO, knockout.
$^{*}P < 0.05$; $^{\dagger}P < 0.01$; $^{\ddagger}P < 0.001$.

to lungs from WT mice (**Fig. 5D**). However, the expressions of CAM-associated genes, including *Il-1b*, *Il-6*, *Il12 p40*, and *iNos,* were comparable (**Fig. 5E**).

https://doi.org/10.4168/aair.2021.13.3.479

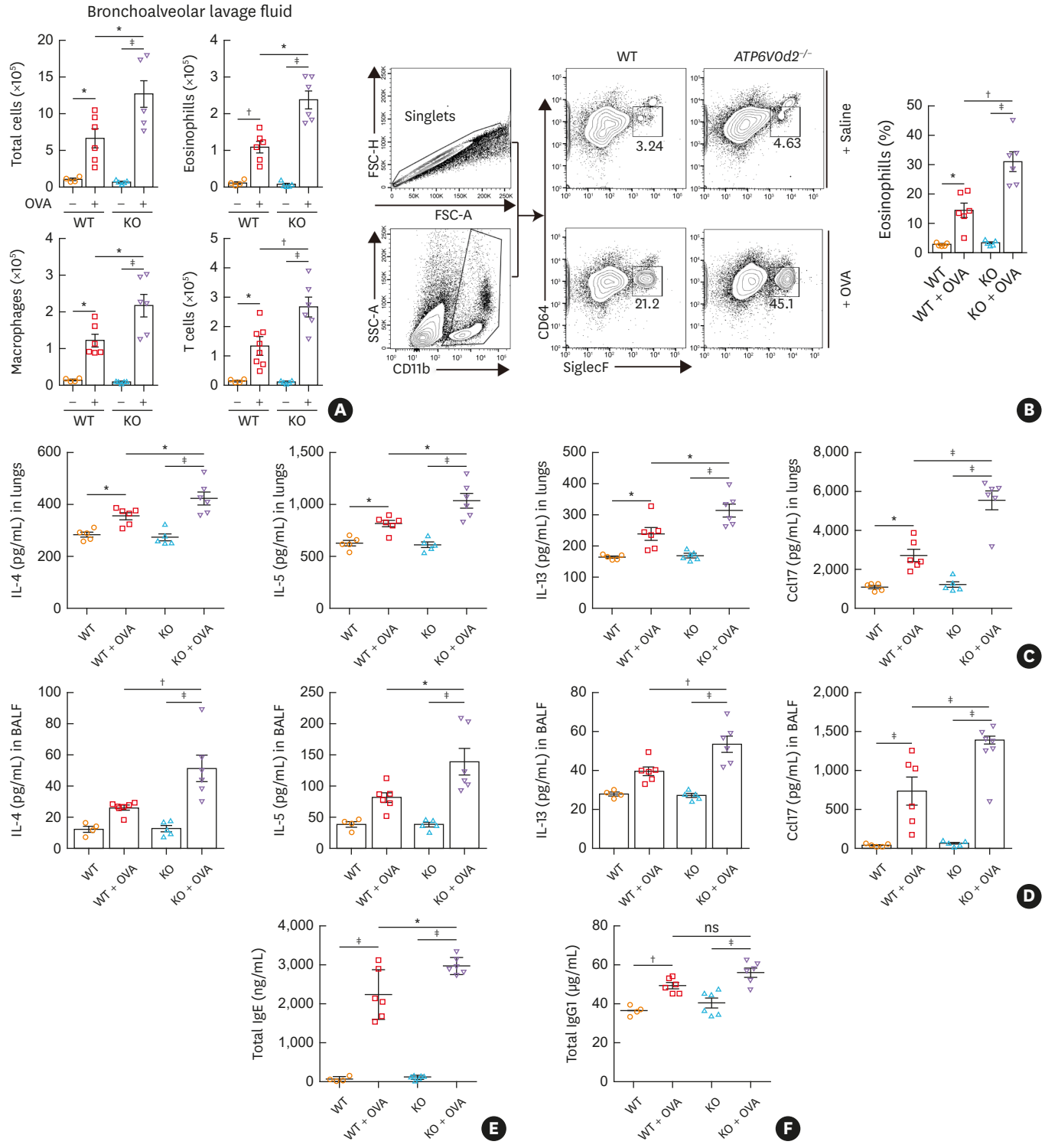

Fig. 4. Deletion of *Atp6v0d2* exacerbated lung inflammation and elevated production of inflammatory mediators upon asthma induction. (A) Numbers of total cells or different types of immune cells, including eosinophils, macrophages, and T cells, in BALF of saline or OVA-treated WT and *ATP6V0d2*$^{-/-}$ mice. (B) Flow cytometry analysis eosinophils in the lungs from WT and *ATP6V0d2*$^{-/-}$ mice after saline or OVA treatment. (C, D) The levels of IL-4, IL-5, IL-13 and Ccl17 in the lungs and BALF, respectively, were determined by ELISA (n = 4–6). (E, F) Serum levels of total IgE and IgG1were determined in WT and *ATP6V0d2*$^{-/-}$ mice treated with saline or OVA using ELISA (n = 4-6). Data are representative of 2 independent experiments. Data were assessed by one-way analysis of variance with Turkey's test and are presented as mean ± standard error of the mean.
BALF, bronchoalveolar lavage fluid; OVA, ovalbumin; WT, wild-type; ELISA, enzyme-linked immunosorbent assay; Ig, immunoglobulin; KO, knockout.
*P < 0.05; †P < 0.01; ‡P < 0.001.

https://doi.org/10.4168/aair.2021.13.3.479

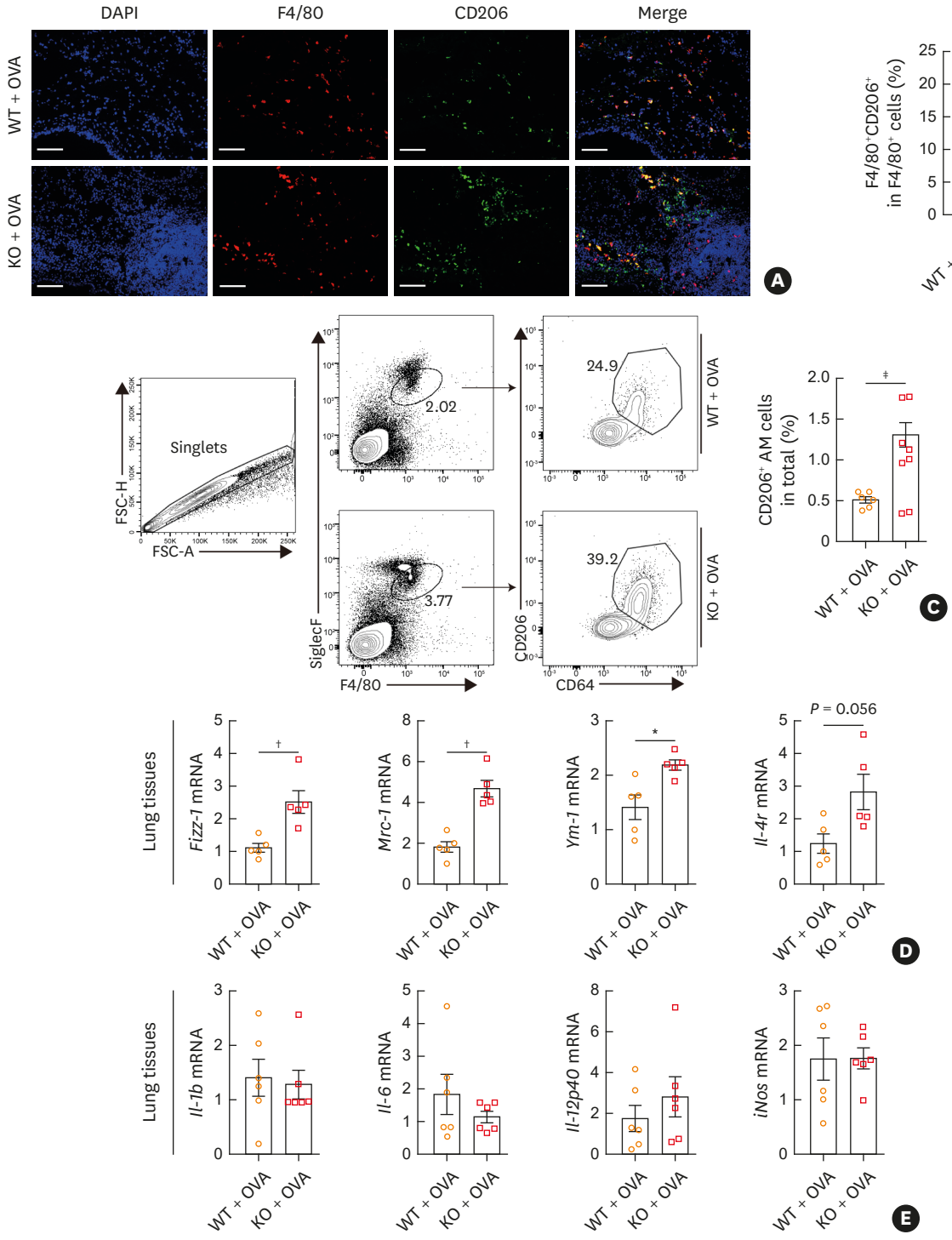

Fig. 5. *ATP6V0d2*-deficiency enhanced AAM polarization in the OVA asthma model. (A, B) Whole-mount immunofluorescence staining of DAPI (blue), F4/80 (red), and CD206 (green) in the lung tissues of WT and *ATP6V0d2*$^{-/-}$ mice treated with OVA and the percentages of F4/80^{+}CD206^{+} among F4/80^{+} were quantified with 2 randomly selected visual fields per slide (n = 5). (C) Flow cytometry analysis of singlets, SiglecF^{+}F4/80^{+}, and CD206^{+}CD64^{+} cells in lungs from OVA-challenged WT and *ATP6V0d2*$^{-/-}$ mice and histogram plots of percentages of CD206^{+}CD64^{+} alveolar macrophages among total cells. (D, E) Expression of AAM-related markers (*Fizz-1*, *Mrc-1*, *Ym-1*, and *Il-4r*) and CAM-related markers (*Il-1b*, *Il-6*, *Il-12p40* and *iNos*) in lungs from OVA-treated WT and *ATP6V0d2*$^{-/-}$ mice was determined by qPCR (n = 4–6) (scale bar: 100 μm). Data are representative of 2 independent experiments and shown as the ratio compared to *Gapdh* to $2^{-\Delta Ct}$ for mRNA levels. Data were assessed by the Mann-Whitney *U* test and are presented as mean ± standard error of the mean.
AAM, alternative activated macrophage; OVA, ovalbumin; DAPI, 4',6-diamidino-2-phenylindole; WT, wild-type; CAM, classic activated macrophage; qPCR, quantitative polymerase chain reaction; KO, knockout.
$^{*}P < 0.05$; $^{\dagger}P < 0.01$; $^{\ddagger}P < 0.001$.

https://doi.org/10.4168/aair.2021.13.3.479

Taken together, these data demonstrate that *ATP6V0d2* intrinsically suppresses AAM polarization in asthma.

ATP6V0d2 promotes Pu.1 lysosomal degradation and suppressed Pu.1-mediated Ccl17 production

Pu.1 acts as a critical transcriptional factor for macrophage alternative polarization and regulates asthma pathology.[14,26] Treatment of IL-4 induced *Pu.1* in AMs (**Fig. 6A**). Consistently, IL-4 also induced enhanced Pu.1 protein level in WT macrophage, however, this phenotype was further increased in the absence of *ATP6V0d2*, although the total and phosphorylated Stat6 levels were comparable (**Supplementary Fig. S4A**), indicating the differential expression of Pu.1 was not due to impaired IL-4 signaling. Thus we asked whether Atp6v0d2 affects Pu.1 stability. In the presence of cycloheximide that blocked protein synthesis, Pu.1 degradation was reduced in the absence of *ATP6V0d2* (**Fig. 6B and C**). Treatment of Bafilomycin, a V-ATPase inhibitor led to accumulation of Pu.1 in WT BMDMs, which was abolished in the absence of *ATP6V0d2* (**Fig. 6D**). Next, we isolated BALF cells, most of which were AMs, from WT mice and treated the cells with IL-4. IL-4-induced Pu.1 was co-localized with lysosomes stained with LysoTracker in WT AMs (**Fig. 6E**) and deletion of *ATP6V0d2* led to significant reduction of co-localizations of Pu.1 with lysosome (**Fig. 6F**). We repeated the same experiments with BMDMs and found similar results (**Supplementary Fig. S4B and C**). Meanwhile, OVA challenge induced Pu.1 expression in the lung tissues of WT mice and this was further potentiated in the *ATP6V0d2*-deficient mice (**Fig. 6G and H**). Immunohistochemistry staining showed similar results (**Supplementary Fig. S4D and E**). We found IL-4 induced *Ccl17* expression in AMs (**Fig. 6I**), which is consistent with previous study showing critical role of Ccl17 for recruitment of Th2 cells into the lungs during asthma.[27] Furthermore, IL-4-induced recruitment of Pu.1 into the *Ccl17* promoter and deletion of *Atp6v0d2* led to enhanced IL-4-induced Ccl17 secretion in BMDMs (**Fig. 6J and K**). Taken together, these data suggest that *ATP6V0d2* promotes Pu.1 lysosomal degradation, thus limiting Ccl17 production and asthma disease severity.

ATP6V0d2 expression is inversely correlated with expression of PU.1 and CCL17 and asthma severity in human patients

Next, we investigated whether the ATP6V0d2-PU.1-CCL17 axis is relevant in human asthma. We compared *PU.1* and *CCL17* mRNA expression in the sputum cells from healthy controls and asthmatic patients and found significantly increased expression of *PU.1* and *CCL17* in the induced sputum from asthmatic patients, compared to those from healthy controls (**Fig. 7A and B**). Using a Pearson correlation assay, we found that *PU.1* and *CCL17* expressions were negatively correlated with *ATP6V0d2* expression (**Fig. 7C and D**), but *PU.1* expression was positively correlated with *CCL17* expression (**Fig. 7E**). More importantly, we found that the disease severity measured by the ratio between forced expiratory volume (FEV1) and forced vital capacity (FVC) (FEV1/FVC, less means severer) was inversely correlated with *ATP6V0d2* expression (**Fig. 7F**), suggesting ATP6V0d2 negatively regulates asthma disease severity. In contrast, the disease severity was positively associated with the expression of *PU.1* and *CCL17* (**Fig. 7G and H**). Taken together, these data suggest that ATP6V0d2-PU.1-CCL17 axis regulates asthma severity in both humans and mice.

https://doi.org/10.4168/aair.2021.13.3.479

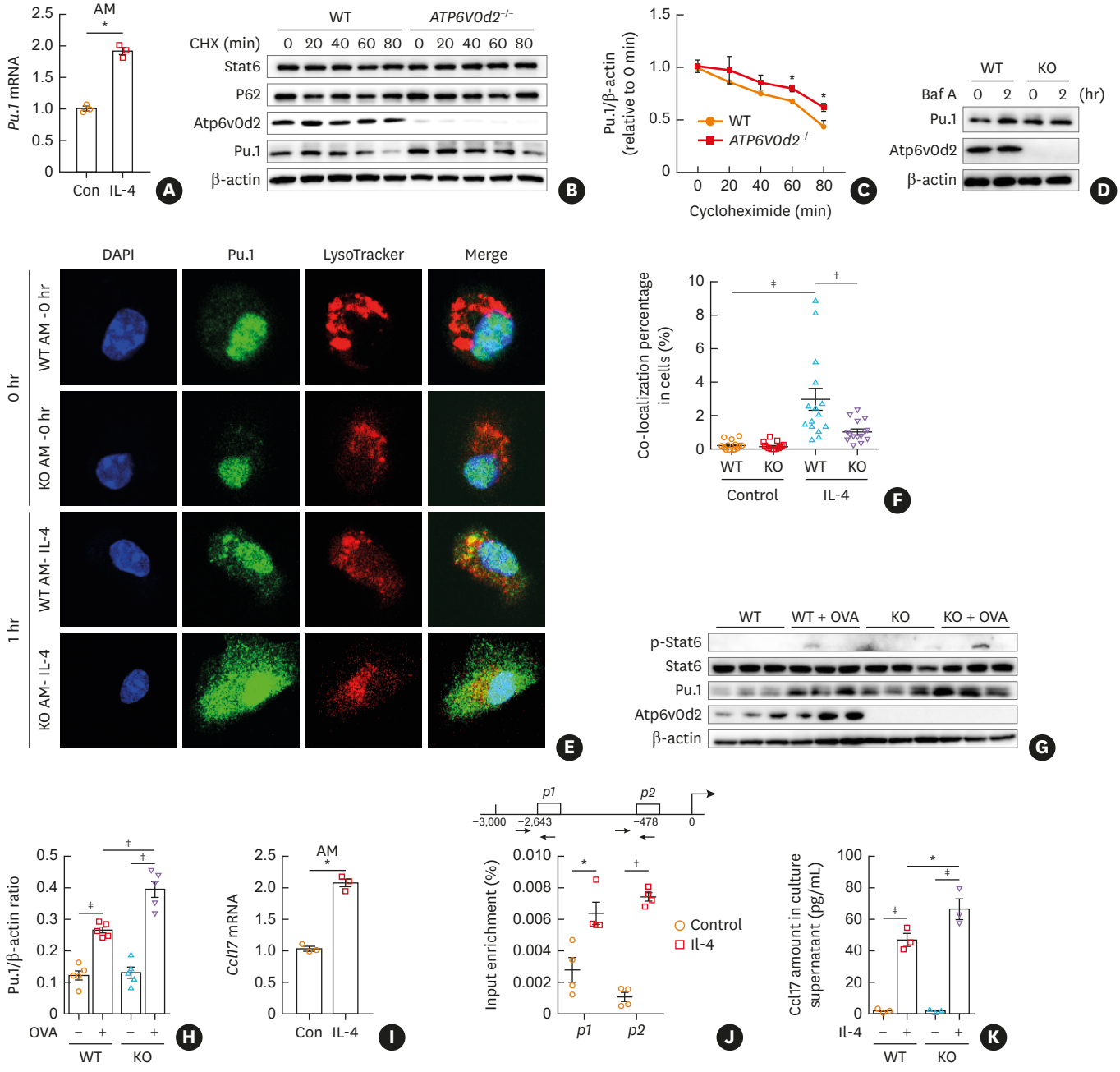

Fig. 6. Deletion of Atp6v0d2 led to Pu.1 accumulation that promotes Ccl17 production. (A) BALF cells isolated from control mice were stimulated with IL-4 (20 ng/mL) for 3 hours and the expression of *Pu.1* was determined by qPCR. (B, C) Immunoblotting of Stat6, P62, Pu.1 and Atp6v0d2 in WT and *ATP6V0d2*$^{-/-}$ BMDMs that were incubated with cycloheximide (100 μg/mL) for the indicated time and band intensities relative to β -actin were plotted. (D) WT and *ATP6V0d2*$^{-/-}$ BMDMs were untreated or treated with bafilomycin A (100 nM) for 2 hours. The amounts of Pu.1 and Atp6v0d2 were determined by immunoblotting. (E, F) BALF cells from control mice were treated with or without IL-4 (20 ng/mL) for 1 hour. Cells were stained with anti-Pu.1 (green) and LysoTracker (red); and percentages of Pu.1 co-localized with LysoTracker among PU.1-positive cells were quantified. Fifteen randomly visual fields were chosen for quantification. (G, H) Immunoblotting of p-Stat6, Stat6, Pu.1 and Atp6v0d2 in lungs from OVA-challenged WT and *ATP6V0d2*$^{-/-}$ mice and the band intensities relative to β -actin were quantified. (I) BALF cells isolated from control mice were stimulated with IL-4 (20 ng/mL) for 3 hours and the expression of *Ccl17* was determined by qPCR. (J) Schematic presentation of the *Ccl17* locus and primers location. The amounts of Pu.1 bound to the *Ccl17* in unstimulated or Il-4 (20 ng/mL, 2h) stimulated WT and *ATP6V0d2*$^{-/-}$ BMDMs were determined by chromatin immunoprecipitation. (K) WT and *Atp6v0d2*$^{-/-}$ BMDMs were stimulated with IL-4 (20 ng/mL) for 48 hours; the amounts of Ccl17 secreted in the supernatants were determined by enzyme-linked immunosorbent assay. Data are representative of 3 independent experiments. Data were assessed by one-way analysis of variance with Turkey's test (F, H, and K) and unpaired Student's *t* test (A, C and I), and are presented as mean ± standard error of the mean.

BALF, bronchoalveolar lavage fluid; qPCR, quantitative polymerase chain reaction; WT, wild-type; BMDM, bone marrow-derived macrophage; KO, knockout.
$^{*}P < 0.05$; $^{\dagger}P < 0.01$; $^{\ddagger}P < 0.001$.

https://doi.org/10.4168/aair.2021.13.3.479

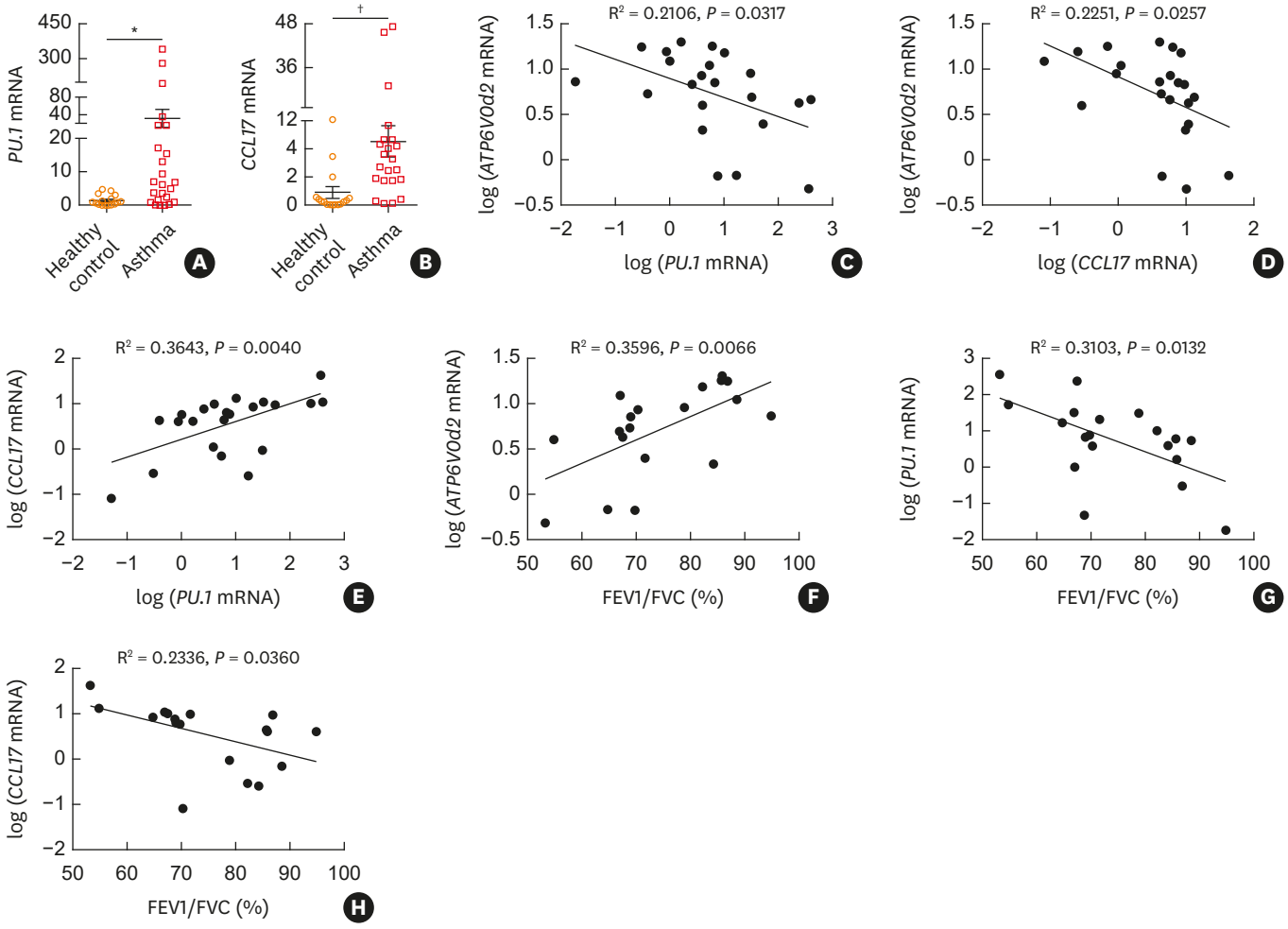

Fig. 7. Data were assessed by one-way ANOVA with Turkey's test (F, H, and K) and unpaired Student's *t*-test (A, C and I), and are presented as mean ± SEM. Expression in induced sputum from patients was inversely associated with the severity of asthma. (A, B) qRCR analysis of *PU.1* and *CCL17* expression in sputum samples from healthy subjects (n = 16) and asthma patients (n = 22). (C-E) Pearson correlation assay for expression of *ATP6V0d2* versus *PU.1*. Data were assessed by one-way ANOVA with Turkey's test (F, H, and K) and unpaired Student's *t*-test (A, C, and I), and are presented as mean ± SEM. *CCL17* and *PU.1* versus *CCL17* in sputum cells from asthma patients. (F-H) Correlation analysis of FEV1/FVC ratio versus expression of *ATP6V0d2*, *PU.1* and *CCL17* in sputum cells from asthmatic patients. Data were assessed by Mann-Whitney *U* test (A, B) and Pearson correlation test (C-G). Data are presented as mean ± SEM.
ANOVA, analysis of variance; SEM, standard error of the mean; FEV1, forced expiratory volume in 1 second; FVC, forced vital capacity.
$^{*}P < 0.05$; $^{\dagger}P < 0.01$.

DISCUSSION

In this study, we found that a subunit of the V-type ATPase pump *ATP6V0d2* is induced during asthma, but serves as an inhibitor of hyperresponsiveness and inflammation in the airway and lung tissues. *ATP6V0d2*-deficient mice had enhanced AAM polarization in an allergic asthma model through reduced degradation of Pu.1. More importantly, *ATP6V0d2* expression was negatively correlated with PU.1 expression and asthma disease severity in humans.

Cellular compositions in sputum and BALF may vary and be affected by age, atopy, and other factors.[28,29] Nevertheless, we found that *ATP6V0d2* expression was enhanced in the induced sputum of asthmatic patients and in the lung tissues of OVA-sensitized mice. In addition, we could recapitulate the induction of Atp6v0d2 by IL-4 in both BALF-derived AMs and BMDMs.

https://doi.org/10.4168/aair.2021.13.3.479

Pu.1 has been shown to promote Th9 differentiation and AAM differentiation, which exacerbates asthma inflammation.[30,31] Deletion of Pu.1 alleviated IL-4-mediated AAM polarization and eosinophilic asthmatic inflammation both *in vitro* and *in vivo*.[14]

In addition, Pu.1 also regulates *Ccl17* expression, which promotes the recruitment of Th2 and Th9 cells into the upper respiratory tracts and further manifests disease severity.[32,33] Consistently, we found Il-4-induced Pu.1 directly binds to *Ccl17* promoter in murine BMDMs. Recently, it has been shown that LPS can enhance Pu.1 binding to *Ccl22* promoter in BMDMs and dendritic cells.[16] However, in our study, we could not find enhanced Pu.1 binding to *Ccl22* locus upon IL-4 treatment (data not shown), indicating differential chromatin conformations of *Ccl22* loci between LPS and IL-4 treatments.

Pu.1 possesses a PEST domain that could be targeted by proteasome degradation; however, truncation of the Pu.1 PEST domain did not lead to protein stabilization suggesting proteasome-independent degradation.[34,35] In line with this, Pu.1 has been shown to be subject to K63 ubiquitination and degradation through p62-dependent autophagy in Th9 cells.[36] Consistent with these, we found that the *ATP6V0d2* mediates Pu.1 degradation in a lysosome-dependent manner. We recently showed that *ATP6V0d2* mediates degradation of hypoxia-inducible factor (HIF)-2α, but not HIF-1α, in tumor- associated macrophages and regulates leucine-induced mTORC1 activation and M2 polarization *in vitro*.[21,22] The molecular mechanisms of how *ATP6V0d2* selectively regulates lysosomal degradation of transcriptional factors under different pathological conditions remain unclear, which warrants further biochemical investigations.

Despite the induction of ATP6V0d2 during asthma, the expression of *ATP6V0d2* was negatively correlated with the asthma severity. It is likely that *ATP6V0d2* acts as a feedback inhibitor for constraining airway hyper-inflammation. Hosts have developed multiple mechanisms for feedback inhibition of inflammation. For example, IL-6 family cytokines induce suppressor of cytokine signaling and IL-1-family cytokines and TLR agonists induce A20, both of which suppress their signaling pathways that initiate their expression.[37,38]

There are at least 3 different types of macrophages including AM, intestinal macrophages and monocyte-derived macrophages in the lung tissues.[39] The polarization of macrophages under different disease conditions adds another layer of complexity to the function of macrophages during asthma. Both protective and pathogenic roles of AAM have been reported in the literature.[40] Our data indicate a pathogenic role of AAMs in asthma and there is a feedback inhibitory pathway by the Atp6v0d2-Pu.1-Ccl17 axis in regulation of AAMs polarization, which is consistent with previous literature.[14,41]

Atp6v0d2 is not expressed in T cells, B cells, and cancer cells in our study.[21] However, we could not completely rule out the possible role of *Atp6v0d2* in other myeloid cells in addition to macrophages. Another limitation of the study is that we could not completely differentiate the tissue-resident AMs and Mo-AMs due to the scarce of the cells. Asthma can be also classified as neutrophils-dominant or eosinophils-dominant types.[29] It remains unclear how *ATP6V0d2* expression regulates the numbers of neutrophils and eosinophils within the respiratory tract and lung tissues. Further studies using sophisticated fate-tracking system of AMs will shed more light on the functions of subpopulations of AMs in the regulation of asthma.

https://doi.org/10.4168/aair.2021.13.3.479

In summary, we uncovered a novel regulatory axis of ATP6V0d2-PU.1-CCL17 in AM polarization, which is associated with human asthma severity.

ACKNOWLEDGMENTS

This work was supported by grants to Xiang-Ping Yang from Key Special Project of Ministry of Science and Technology (2019YFC1316203) and the National Scientific Foundation of China to Xiang-Ping Yang (81671539, 31870892), National Natural Science Foundation of China (NSFC) grant to Huabin Li (81725004), Guohua Zhen (81670019, 91742108).

SUPPLEMENTARY MATERIALS

Supplementary Table S1

Characteristics of the study subjects

Click here to view

Supplementary Table S2

Primer sequences for PCR

Click here to view

Supplementary Fig. S1

The cellular compositions of induced sputum cells from healthy and asthma patients and in BALF supernatants from control mice. (A) Representative flow cytometry analysis of $CD33^+$ neutrophils, $CD68^+$ macrophages, $CD3^+$ T cells and $CD19^+$ B cells in the sputum cells of induced saliva from healthy controls and asthma patients. (B) Flow cytometry analysis of alveolar macrophage in BALF from control mice.

Click here to view

Supplementary Fig. S2

Atp6v0d2 expression is counter regulated by IL-4 and LPS. (A) Immunoblotting of p-NF-κB, Atp6v0d2, Atp6v0d1 and Atp6v1a in WT BMDMs stimulated with LPS (100 ng/mL) for the indicated times. (B) *Atp6v0d2* expression was determined by qPCR in BMDMs stimulated with LPS alone or with the addition of NF-κB inhibitor BAY11-7082 (5 μM). (C, D) BMDMs were stimulated with Il-4 (20 ng/mL) for 24 hours or in combination with increasing amounts of LPS, then *Atp6v0d2* expression was detected by qPCR and western blot. (E, F) BMDMs were stimulated with LPS (100 ng/mL) for 24 hours or in combination with increasing amounts of IL-4, then the *Atp6v0d2* expression was detected by qPCR and western blot. Data are representative of three independent experiments. Data were assessed by one-way analysis of variance with Turkey's test and presented as mean ± standard error of the mean.

Click here to view

Supplementary Fig. S3

OVA challenged *ATP6V0d2*$^{-/-}$ mice does not affect B cells infiltration or IL-6 and IL-10 production compared to WT mice. (A) Flow cytometry analysis of CD3^{+} cells and CD19^{+} cells in lung tissues and histogram comparison of fractions of CD3^{+} and CD19^{+} cells from saline or OVA-treated WT and *Atp6v0d2*$^{-/-}$ mice. (B, C) Comparison of the IL-6 and IL-10 levels in the lungs and BALF supernatants from saline- or OVA-treated WT and *ATP6V0d2*$^{-/-}$ mice. Data are representative of 2 independent experiments. Data were assessed by one-way analysis of variance with Turkey's test and presented as mean ± standard error of the mean.

Click here to view

Supplementary Fig. S4

Deletion of *Atp6v0d2* results in enhanced Pu.1 expression. (A) The levels of p-Stat6, Stat6, Pu.1 and Atp6v0d2 were determined by immunoblotting analysis in WT and *ATP6V0d2*$^{-/-}$ BMDMs that were stimulated with IL-4 (20 ng/mL) for the indicated times. (B, C) WT and *Atp6v0d2*$^{-/-}$ BMDMs were treated with or without IL-4 (20 ng/mL) for 2 hours. Cells were stained with anti-Pu.1 (green) and LysoTracker (red) and percentages of Pu.1 co-localized with LysoTracker among Pu.1-positive cells were quantified. (D) Representative images of IHC analysis of Pu.1 expression in lung tissues from saline- or OVA-treated WT and *Atp6v0d2*$^{-/-}$ mice and quantification of the percentages of Pu.1-positive cells (scale bar: 100 μm). Data are representative of two independent experiments. Data were assessed by one-way analysis of variance with Turkey's test and presented as mean ± standard error of the mean.

Click here to view

REFERENCES

1. Lambrecht BN, Hammad H. The immunology of asthma. Nat Immunol 2015;16:45-56.
PUBMED | CROSSREF
2. Mukherjee M, Nair P. Autoimmune responses in severe asthma. Allergy Asthma Immunol Res 2018;10:428-47.
PUBMED | CROSSREF
3. Byrne AJ, Mathie SA, Gregory LG, Lloyd CM. Pulmonary macrophages: key players in the innate defence of the airways. Thorax 2015;70:1189-96.
PUBMED | CROSSREF
4. Fricker M, Gibson PG. Macrophage dysfunction in the pathogenesis and treatment of asthma. Eur Respir J 2017;50:1700196.
PUBMED | CROSSREF
5. Zasłona Z, Przybranowski S, Wilke C, van Rooijen N, Teitz-Tennenbaum S, Osterholzer JJ, et al. Resident alveolar macrophages suppress, whereas recruited monocytes promote, allergic lung inflammation in murine models of asthma. J Immunol 2014;193:4245-53.
PUBMED | CROSSREF
6. Balhara J, Gounni AS. The alveolar macrophages in asthma: a double-edged sword. Mucosal Immunol 2012;5:605-9.
PUBMED | CROSSREF
7. Tsou CL, Peters W, Si Y, Slaymaker S, Aslanian AM, Weisberg SP, et al. Critical roles for CCR2 and MCP-3 in monocyte mobilization from bone marrow and recruitment to inflammatory sites. J Clin Invest 2007;117:902-9.
PUBMED | CROSSREF
8. Shi C, Pamer EG. Monocyte recruitment during infection and inflammation. Nat Rev Immunol 2011;11:762-74.
PUBMED | CROSSREF

9. Misharin AV, Morales-Nebreda L, Reyfman PA, Cuda CM, Walter JM, McQuattie-Pimentel AC, et al. Monocyte-derived alveolar macrophages drive lung fibrosis and persist in the lung over the life span. J Exp Med 2017;214:2387-404.
PUBMED | CROSSREF

10. Gundra UM, Girgis NM, Gonzalez MA, San Tang M, Van Der Zande HJ, Lin JD, et al. Vitamin A mediates conversion of monocyte-derived macrophages into tissue-resident macrophages during alternative activation. Nat Immunol 2017;18:642-53.
PUBMED | CROSSREF

11. Gordon S, Martinez FO. Alternative activation of macrophages: mechanism and functions. Immunity 2010;32:593-604.
PUBMED | CROSSREF

12. Murray PJ. Macrophage polarization. Annu Rev Physiol 2017;79:541-66.
PUBMED | CROSSREF

13. Lawrence T, Natoli G. Transcriptional regulation of macrophage polarization: enabling diversity with identity. Nat Rev Immunol 2011;11:750-61.
PUBMED | CROSSREF

14. Qian F, Deng J, Lee YG, Zhu J, Karpurapu M, Chung S, et al. The transcription factor PU.1 promotes alternative macrophage polarization and asthmatic airway inflammation. J Mol Cell Biol 2015;7:557-67.
PUBMED | CROSSREF

15. Uhm TG, Kim BS, Chung IY. Eosinophil development, regulation of eosinophil-specific genes, and role of eosinophils in the pathogenesis of asthma. Allergy Asthma Immunol Res 2012;4:68-79.
PUBMED | CROSSREF

16. Yashiro T, Nakano S, Nomura K, Uchida Y, Kasakura K, Nishiyama C. A transcription factor PU.1 is critical for Ccl22 gene expression in dendritic cells and macrophages. Sci Rep 2019;9:1161.
PUBMED | CROSSREF

17. Girodet PO, Nguyen D, Mancini JD, Hundal M, Zhou X, Israel E, et al. Alternative macrophage activation is increased in asthma. Am J Respir Cell Mol Biol 2016;55:467-75.
PUBMED | CROSSREF

18. Bagh MB, Peng S, Chandra G, Zhang Z, Singh SP, Pattabiraman N, et al. Misrouting of v-ATPase subunit V0a1 dysregulates lysosomal acidification in a neurodegenerative lysosomal storage disease model. Nat Commun 2017;8:14612.
PUBMED | CROSSREF

19. Mauvezin C, Neufeld TP. Bafilomycin A1 disrupts autophagic flux by inhibiting both V-ATPase-dependent acidification and Ca-P60A/SERCA-dependent autophagosome-lysosome fusion. Autophagy 2015;11:1437-8.
PUBMED | CROSSREF

20. Xia Y, Liu N, Xie X, Bi G, Ba H, Li L, et al. The macrophage-specific V-ATPase subunit ATP6V0D2 restricts inflammasome activation and bacterial infection by facilitating autophagosome-lysosome fusion. Autophagy 2019;15:960-75.
PUBMED | CROSSREF

21. Liu N, Luo J, Kuang D, Xu S, Duan Y, Xia Y, et al. Lactate inhibits ATP6V0d2 expression in tumor-associated macrophages to promote HIF-2α-mediated tumor progression. J Clin Invest 2019;129:631-46.
PUBMED | CROSSREF

22. Li P, Deng X, Luo J, Chen Y, Bi G, Gong F, et al. ATP6V0d2 mediates leucine-induced mTORC1 activation and polarization of macrophages. Protein Cell 2019;10:615-9.
PUBMED | CROSSREF

23. Reddel HK, Taylor DR, Bateman ED, Boulet LP, Boushey HA, Busse WW, et al.. An official American Thoracic Society/European Respiratory Society statement: asthma control and exacerbations: standardizing endpoints for clinical asthma trials and clinical practice. Am J Respir Crit Care Med 2009;180:59-99.
PUBMED | CROSSREF

24. Hunter CJ, Ward R, Woltmann G, Wardlaw AJ, Pavord ID. The safety and success rate of sputum induction using a low output ultrasonic nebuliser. Respir Med 1999;93:345-8.
PUBMED | CROSSREF

25. Wang Y, Zhu J, Zhang L, Zhang Z, He L, Mou Y, et al. Role of C/EBP homologous protein and endoplasmic reticulum stress in asthma exacerbation by regulating the IL-4/signal transducer and activator of transcription 6/transcription factor EC/IL-4 receptor α positive feedback loop in M2 macrophages. J Allergy Clin Immunol 2017;140:1550-1561.e8.
PUBMED | CROSSREF

26. Jego G, Lanneau D, De Thonel A, Berthenet K, Hazoumé A, Droin N, et al. Dual regulation of SPI1/PU.1 transcription factor by heat shock factor 1 (HSF1) during macrophage differentiation of monocytes. Leukemia 2014;28:1676-86.
PUBMED | CROSSREF

27. Medoff BD, Seung E, Hong S, Thomas SY, Sandall BP, Duffield JS, et al. CD11b+ myeloid cells are the key mediators of Th2 cell homing into the airway in allergic inflammation. J Immunol 2009;182:623-35.
PUBMED | CROSSREF

28. Balbi B, Pignatti P, Corradi M, Baiardi P, Bianchi L, Brunetti G, et al. Bronchoalveolar lavage, sputum and exhaled clinically relevant inflammatory markers: values in healthy adults. Eur Respir J 2007;30:769-81.
PUBMED | CROSSREF

29. Son JH, Kim JH, Chang HS, Park JS, Park CS. Relationship of microbial profile with airway immune response in eosinophilic or neutrophilic inflammation of asthmatics. Allergy Asthma Immunol Res 2020;12:412-29.
PUBMED | CROSSREF

30. Gerlach K, Hwang Y, Nikolaev A, Atreya R, Dornhoff H, Steiner S, et al. TH9 cells that express the transcription factor PU.1 drive T cell-mediated colitis via IL-9 receptor signaling in intestinal epithelial cells. Nat Immunol 2014;15:676-86.
PUBMED | CROSSREF

31. Koch S, Sopel N, Finotto S. Th9 and other IL-9-producing cells in allergic asthma. Semin Immunopathol 2017;39:55-68.
PUBMED | CROSSREF

32. Chang HC, Sehra S, Goswami R, Yao W, Yu Q, Stritesky GL, et al. The transcription factor PU.1 is required for the development of IL-9-producing T cells and allergic inflammation. Nat Immunol 2010;11:527-34.
PUBMED | CROSSREF

33. Vijayanand P, Durkin K, Hartmann G, Morjaria J, Seumois G, Staples KJ, et al. Chemokine receptor 4 plays a key role in T cell recruitment into the airways of asthmatic patients. J Immunol 2010;184:4568-74.
PUBMED | CROSSREF

34. Nishiyama C, Nishiyama M, Ito T, Masaki S, Masuoka N, Yamane H, et al. Functional analysis of PU.1 domains in monocyte-specific gene regulation. FEBS Lett 2004;561:63-8.
PUBMED | CROSSREF

35. Konishi Y, Tominaga A. PU.1 is degraded in differentiation of erythrocytes through a proteasome-dependent pathway. DNA Cell Biol 2006;25:340-5.
PUBMED | CROSSREF

36. Rivera Vargas T, Cai Z, Shen Y, Dosset M, Benoit-Lizon I, Martin T, et al. Selective degradation of PU.1 during autophagy represses the differentiation and antitumour activity of T_H9 cells. Nat Commun 2017;8:559.
PUBMED | CROSSREF

37. Babon JJ, Varghese LN, Nicola NA. Inhibition of IL-6 family cytokines by SOCS3. Semin Immunol 2014;26:13-9.
PUBMED | CROSSREF

38. Dinarello CA. Overview of the IL-1 family in innate inflammation and acquired immunity. Immunol Rev 2018;281:8-27.
PUBMED | CROSSREF

39. Puttur F, Gregory LG, Lloyd CM. Airway macrophages as the guardians of tissue repair in the lung. Immunol Cell Biol 2019;97:246-57.
PUBMED | CROSSREF

40. Abdelaziz MH, Abdelwahab SF, Wan J, Cai W, Huixuan W, Jianjun C, et al. Alternatively activated macrophages; a double-edged sword in allergic asthma. J Transl Med 2020;18:58.
PUBMED | CROSSREF

41. Staples KJ, Hinks TS, Ward JA, Gunn V, Smith C, Djukanović R. Phenotypic characterization of lung macrophages in asthmatic patients: overexpression of CCL17. J Allergy Clin Immunol 2012;130:1404-1412.e7.
PUBMED | CROSSREF